Pinning of interfaces by three-dimensional potentials

1999 J. Phys.: Condens. Matter 11 2719

(http://iopscience.iop.org/0953-8984/11/13/009)

J. Phys.: Condens. Matter **11** (1999) 2719–2727. Printed in the UK PII: S0953-8984(99)97591-4

Pinning of interfaces by three-dimensional potentials

S T Chui

Bartol Research Institute, University of Delaware, Newark, DE 19716, USA

Received 25 September 1998, in final form 30 November 1998

Abstract. We study two models for the depinning of a two-dimensional interface by *finite* external forces from a three-dimensional potential in the context of spin systems. This type of model is motivated by an attempt to understand better the pinning of domain walls in magnets and represents a new direction in the study of the pinning of walls. A simple analytic model is proposed that provides for a semi-quantitative interpretation of results from Monte Carlo simulations. The optimization of the depinning field at a finite temperature involves a compromise between the cell boundary width and the cell pinning strength.

1. Introduction

Within the last twenty years, there has been much work on the physics of interfaces (domain walls) in the context of the roughening, wetting and depinning transitions [1–5]. These investigations have focused on the statistical mechanics of a two-dimensional interface in the presence of external potentials of different forms. In the roughening transition, the 'pinning potential' is uniform in the xy-plane but periodic in the z-direction. In the wetting transition, the external potential is localized in the z-direction and uniform in the xy-direction. In these previous studies, most of the interest was focused on the regime of linear response, for which the external depinning field is small. In this paper we study models such that the external potential can be periodic in all three directions and focus on the regime in which the depinning field is no longer small.

These models are motivated by our desire to understand the fundamental physics of the pinning of domain walls in the $Sm(Co, Fe, Cu, Zr)_z$ (2:17) permanent magnets. The development of 2:17 permanent magnets was the result of intensive research in the late 1960s and 1970s [6,7]. Those studies suggest that the optimum material consists of a network of small cells separated by cell boundaries of the order of ten lattice spacings wide that are approximately of $SmCo_5$ stoichiometry. Lorentz microscopy suggests that the magnetic domain walls are pinned at the cell boundaries.

The pinning potentials that we have looked at in this paper are localized at the faces of a periodic array of cubes and at a periodic arrays of planes. *Finite-temperature* Monte Carlo simulations and simple analytic calculations were performed to clarify the depinning of magnetic domain walls by an external field from the three-dimensional model 'cell' structures. We hope that our work will provide a foundation based on which more sophisticated calculations can be performed. Our simulation was carried out on a 3D Heisenberg model with a uniaxial anisotropy and with cubic cells under periodic boundary conditions. The anisotropy constant and/or the exchange inside the cell boundaries is assumed to be smaller than that in the bulk by a reduction factor r^2.

0953-8984/99/132719+09$19.50

We found that the temperature dependence of the depinning field is very strong when the anisotropy constant of the cell boundary is close to that of the bulk. This seems to be the case for the existing commercial magnets. On the other hand, the temperature dependence is much weaker when the cell boundary becomes substantially different from that of the bulk. Thus to optimize the depinning field at a finite temperature, one should design materials with a slow enough temperature dependence, at the expense of a lower low-temperature switching field, that the high-temperature depinning field can be maximized. Samples recently made by Kim [8] and by Liu and co-workers [9–11] exhibit a slower temperature dependence of the depinning field and are consistent with this picture.

Examination of the spin configuration during reversal suggests a nucleation-type process with kinks in the magnetic domain wall created at the corners of the cell structures. Motivated by the past work on the mechanisms of the pinning of interfaces such as the wetting transition [3,5], we propose an analytic model to explain the essential physics of the nucleation process in such a case and find a *low*-temperature dependence of the depinning field given approximately by

$$H_c(T)/H_c(0) = 1 - c(T/l(\Delta\sqrt{KJ}))^{0.5}$$

for some constant c. This scaling seems to be obeyed quite well when compared with the simulation results. In real materials there may be an additional temperature dependence, electronic in origin, which changes the parameters used in the present discussion. We also found that the dependence of the depinning field on some of the system parameters for models with 3D cell boundaries differs qualitatively from that derived from models based on pinning by 2D boundaries. We now explain our results in detail.

2. The model

Our model consists of Heisenberg spins interacting with each other with short-range exchange and on-site uniaxial anisotropy interactions in a box of size $L_1 \times L_2 \times L_3$ under periodic boundary conditions. The energy of interaction between the spins at the positions $\boldsymbol{R}$, $\boldsymbol{R}'$ is

$$U = 0.5 \sum_{ij=xyz,\boldsymbol{R}\boldsymbol{R}'} V_{ij}(\boldsymbol{R}-\boldsymbol{R}')S_i(\boldsymbol{R})S_j(\boldsymbol{R}')$$

where $V = V_d + V_e + V_a$ is the sum of: the dipolar energy $V_{dij}(\boldsymbol{R}) = g\nabla_i\nabla_j(1/|\boldsymbol{R}|)$; the exchange energy $V_e = -J\delta(\boldsymbol{R}=\boldsymbol{R}'+a)\delta_{ij}$; and the crystalline anisotropy energy

$$V_a = -2K\sum_i S_{ix}^2.$$

Here a denotes the nearest-neighbour distance. g and J are coupling constants. We have performed calculations for both cell defects and planar defects. The cell defect structure is modelled by cell boundaries of thickness l centred at $z = 0$ and at $x = L_1/2$, $y = L_2/2$ or $z = L_3/2$. The spins inside the cell boundaries are assumed to exhibit an anisotropy constant that is reduced from the bulk value by a factor r^2. Lorentz microscopy shows that for the optimal magnets part of the magnetic domain wall lies *parallel* to the cell boundaries [17]. This implies an *attractive* potential which pins the domain wall inside the cell boundaries with the result that the anisotropy constant and/or the exchange inside the cell boundaries is smaller than that in the bulk by a factor $r^2 < 1$. Recently, a two-dimensional analysis of the energy of different pinning configurations for a model for the 2:17 material was studied by Katter [18]. This model assumes a *repulsive* cell boundary and thus is not appropriate for the optimum magnets. We have also performed calculations where the exchange is also reduced at the cell boundary. The results are similar. Since we do not yet know what the experimental reduction

factor actually is, to keep the length of the paper down, we shall mostly focus on the case where only K is changed. The planar defect is modelled with defect walls only centred at $z = 0$ and at $z = L_3/2$.

Our simulation follows our recent finite-temperature studies of ultra-thin films [15]. This technique reproduces known micromagnetics results and avoids some of the pitfalls of zero-temperature calculations such as getting stuck in local metastable states. The largest system that we looked at consists of 128 000 spins. This is about double the size of systems investigated in previous zero-temperature micromagnetics calculations for the nanocomposite NdFeB magnets [16]. Because of the long-range nature of the dipolar potential, the present calculation is more challenging than that with short-range interactions.

Our Monte Carlo (MC) simulation uses the well established Metropolis algorithm [19]. Most micromagnetics calculation solves the Landau–Gilbert equation at *zero temperature*. The MC simulation corresponds to solving the master equation. We expect this dynamics to produce the correct free energy of nucleation and coercive field but a prefactor in the nucleation rate that may be different from that of a stochastic Landau–Gilbert equation. Our finite-temperature MC simulation produces results in agreement with theoretical predictions in micromagnetics in all of the cases that we have investigated [20].

Most of our calculations are performed for $L_1 = L_2 = L_3/2 = 20$. For the sake of simplicity we assumed that the spins reside on a simple cubic lattice. At the beginning, at zero external field, the spins with $z \leqslant 0$ and $z > 0$ are assumed to point in opposite x-directions.

Monte Carlo calculations are performed so that an equilibrium configuration is reached. External fields of different magnitudes along the x-direction are then applied. The magnetization is sampled and averaged every 200 MC steps/spin. If the change is larger than the standard deviation after 4000 MC steps/spin, the simulation is repeated until the magnetization is finally stabilized. The depinning field is determined by that which causes the onset of spin reversal. We next discuss the choice of the interaction parameters.

For Sm_2Co_{17}, $T_c = 1193$ K; thus the bare exchange $J_0 \approx T_c/1.5 = 800$ K [12]. The anisotropy constant is $K_1 = 3.2 \times 10^7$ erg cm^{-3} and the volume per unit cell is $v = 787$ Å^3 [7]; thus the anisotropy energy per unit cell K_0 is $K_1 v = 182$ K. The magnetization is $M_s = 12.5$ kG$/4\pi \approx 10^3$ G; thus the effective dipolar coupling is $g_0 = M_s^2 v \approx 5.7$ K. $J_0/K_0 = 4.4$, $J_0/g_0 = 140$. The pinning cell boundary width is about 40 Å whereas the lattice constant is about 8 Å. Thus the boundary width is about five times the lattice constant. For the experimental systems, J is larger than g and K. Thus over short length scales at a low enough temperature, the spins are aligned. It is possible to describe the system in terms of block spins with renormalized interactions. This facilitates the simulation of the formation of domain walls in a system of reasonable size. In this paper, we shall assume that we are dealing with block spins that each consist of d^3 atomic spins. For block spins of d^3 unit cells, the anisotropy, exchange and dipolar interactions are scaled approximately as $K = K_0 d^3$, $J = J_0 d$ and $g = g_0 d^3$. If we take a block spin with eight unit cells, then $J/K \approx 1$, $J_0/g_0 = 35$. In this paper we have performed simulations with $K = -5.5$ and $J = -10$ ($J/K \approx 2$) and $J = -20$ ($J/K \approx 4$). We have carried out calculations with g ranging from 0 to 1 and found no difference in our results. This is in contrast with the case for Nd–Fe–B magnets where the dipolar effects can be more important because of the existence of the soft phase in the 'nanocomposite'.

3. Simulation results

The temperature dependence of the depinning field of our model is shown in figure 1 for different cell boundary widths $l = 3, 5, 10$ and for different reduction factors $r = 0.7, 0.9$.

The top dashed curve is for pinning by 2D planar boundaries. Most of our calculations are carried out for $20 \times 20 \times 40$ spins. To minimize finite-size effects, the results for the largest l that we have examined, $l = 10$, are carried out for a larger system with $40 \times 40 \times 80$ spins. The simulation result for the switching field is smaller than that for the anisotropy field by one order of magnitude, which is the same situation as for the experimental systems. This is reasonable because the pinning potential is controlled by the *difference* between the domain wall energies inside and outside the pinning boundaries, as we discuss in detail in the next section. The dashed–triple-dotted curve is for $r = 0.9$ whereas the other curves are for $r = 0.7$.

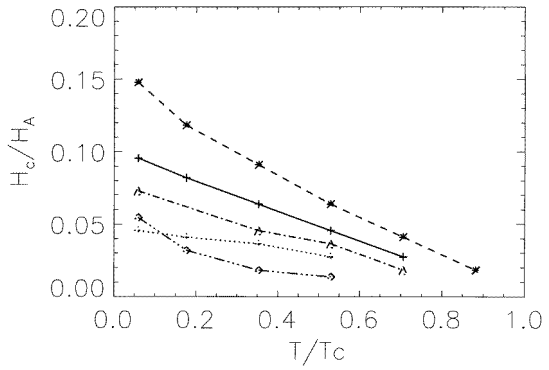

Figure 1. The switching fields normalized by the anisotropy field $H_A = 2$ K as a function of temperature normalized by $T_c \approx 1.7J$. $J = 10$. The solid, dotted–dashed and dotted curves are for $r = 0.7$ and for $l = 3$, 5 and 10. The dashed–triple-dotted curve is for $r = 0.9$ and $l = 5$. The dashed curve is for a planar defect with $l = 3$ and $r = 0.7$.

The temperature dependence is stronger when the anisotropy constant of the cell boundary is closer to that of the bulk (see the dashed–triple-dotted curve at the bottom for $r = 0.9$). This seems to be the case for the existing commercial magnets. On the other hand, the temperature dependence is much weaker when the cell boundary becomes substantially different from the bulk. Thus to optimize the depinning field at a finite temperature, one should design materials with a slow enough temperature dependence, at the expense of a lower low-temperature switching field, that the high-temperature depinning field can be maximized. Samples recently made by Kim [8] and by Liu and co-workers [9–11] exhibit a slower temperature dependence of the depinning field and are consistent with this picture. Most previous theoretical work [13,14] has focused on the depinning from planar defects at zero temperature. For comparison, we have also carried out finite-temperature calculations for the depinning from planar defects. The results are shown by the dashed curve for $r = 0.7$. The temperature dependence is quite fast.

In figure 2 we plot the low-temperature ($T/J = 0.1$) depinning field for different defect configurations and different boundary thicknesses as functions of the square root of the difference of the domain wall energy $\sqrt{\Delta(JK)^{0.5}}$ at the cell boundaries. The particular dependence chosen was suggested by our simple analytic model described in the next section. The fit works reasonably well. When both J and K are reduced at the boundary, the switching field is higher. We found that the depinning field for 2D planar defects is higher than that for 3D cell defects. The dependence of the switching field on the cell boundary thickness is illustrated in figure 3. For planar defects, when the defect width l becomes larger than the magnetic domain wall width $w_0 = \sqrt{(J/K)}$, the depinning field *increases* and approaches a *finite* value. However, for cell defects, as the cell boundary width becomes larger, the depinning field *decreases* to *zero*. As the cell boundary width decreases and eventually becomes small

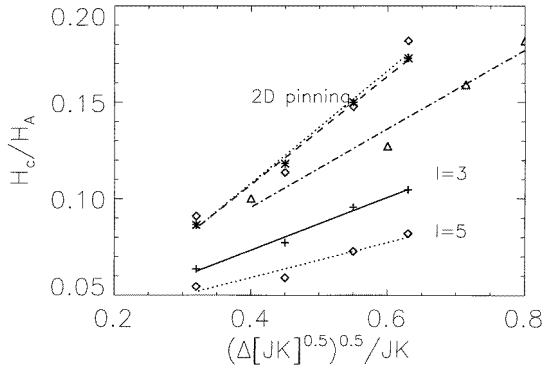

Figure 2. The switching field normalized by the anisotropy field $H_A = 2$ K as a function of the square root of the normalized pinning energy which is proportional to the square root of the difference between the domain wall energies inside and outside the pinning boundaries: $V \propto [(1-r)(JK)^{0.5}]^{0.5}$. The solid and dotted curves are for $l = 3$ and 5. The bottom (top) two curves are for 3D cell (2D planar) pinning when only the anisotropy is changed. The triangles and the dotted–dashed curve are for $l = 3$ when both the anisotropy and the exchange are reduced at the cell boundary. The curves are least-squares fits to the points.

enough compared with the domain wall width, the depinning field decreases to zero for both planar pinning and 3D cell pinning. Thus for cell pinning, there is a maximum in the low-temperature depinning field when the domain wall width is comparable to the cell boundary width. We next examine the physics of the wall depinning.

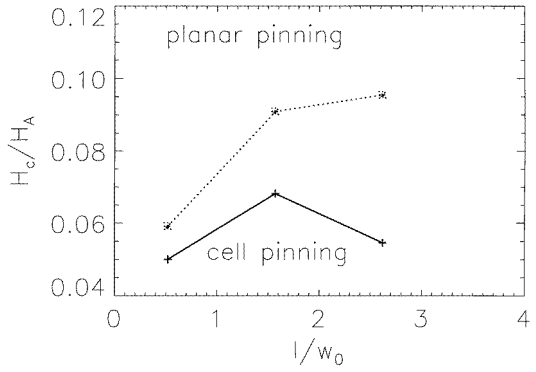

Figure 3. The switching field normalized by the anisotropy field $H_A = 2$ K as a function of the boundary width for planar and for 3D cell pinning for $T/T_c = 0.35$. $J = 20$. K and g are as specified in the text. The error in $H_c/2$ K is 0.004.

A slice of the projection of the spin onto the xy-plane for those spins at $y = 0$ and $z \geqslant 0$ during a reversal process is shown in figure 4. In this picture, the cell boundaries are near the centre at $x = 10$ and near the top and bottom of the figure. Initially all spins point to the right. A magnetic field is applied pointing to the left. Two domain boundaries near the top and the bottom can be seen. Near $x = 10$, these domain walls are curved, protruding a little into the middle. For example, at $y = 7$, the magnitudes of these xy-projections of the spins at $x = 6$ to $x = 13$ are smaller than those outside this region. Similar results can also be seen at $y = 16$. This suggests a picture of reversal whereby kinks in the domain wall nucleate near

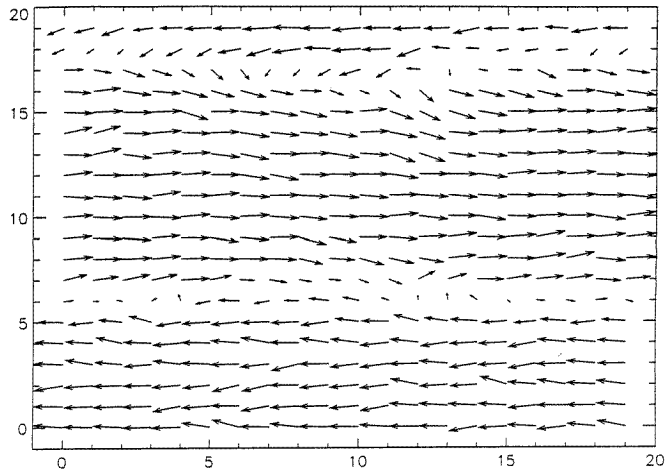

Figure 4. The xy-projection of the spins for a slice of a typical spin configuration for those spins at $y = 0$ and $z \geqslant 0$ during a reversal process for $l = 3$, $T/T_c = 0.35$, and other parameters as specified in the text.

the defect cell corners ($x = 10$) and move outwards. We next describe our attempt to model this nucleation picture analytically.

4. The analytic model

There has been much work on the physics of interfaces (domain walls) within the last twenty years in the context of the roughening, wetting and depinning transitions [1–5]. These investigations have focused on the statistical mechanics of a two-dimensional interface in the presence of external potentials of different forms. In the present case, the domain wall can be considered to be an interface between the spin-up and spin-down regions. We follow these interface investigations and model the current system by considering a phenomenological energy of an interface given by

$$E = \int \mathrm{d}^2 r_\perp \, \sigma (\nabla h)^2 + V\theta(|r_\perp| > l)\theta(h > 0) - Hh(r_\perp).$$

Here h describes the height of the domain wall as a function of its location in the xy-plane (the $r_\perp$-plane). l is the width of the pinning cell. σ is the 'surface tension' of the wall, which is of the order of $r\sqrt{JK}$ [1, 2]. For example, it can come from the increase in the wall area when the wall is curved. There is an additional contribution from the dipolar interaction [1] but it is small in the present case and so is neglected. V is the pinning potential. We focus on a single corner for the cell boundaries and assume the interaction energy between the domain walls at different corners to be small. We assume that when the wall moves away from the pinning cell corner described by the geometrical constraint $\theta(|r_\perp| > l)\theta(h > 0)$, this pinning energy is lost. The pinning discussed here is different from that due to point hard pins. When the domain wall width is less than the cell boundary width, V is of the order of the difference in domain wall energy across the cell boundary $\Delta\sqrt{JK}$. When the domain wall width is larger than l, V decreases and approaches zero [14]. The pinning energy is increased when that part of the interface outside the cell boundary at $r_\perp > l$ is moved up. The depinning occurs through the creation of a 'bubble' inside the cell corners at $r = 0$. This bubble expands sideways and

eventually overcomes the nucleation barrier as the external field is increased. We now try to describe this mathematically.

In the presence of an external field, we expect h to become nonzero with a profile of height a and width b localized around the origin. The strain energy

$$\int \mathrm{d}^2 r\ (\nabla h)^2$$

is of the order of $\sigma b^2 (a/b)^2$. The energy change is of the order of $E = \sigma a^2 + E_p - \alpha H a b^2$ where α is a constant of the order of unity. E_p is the pinning energy. $E_p = 0$ when $b < l$. When $b > l$, the pinning term becomes nonzero: $E_p \approx V(b^2 - l^2)$. The extremum energy can be obtained by setting the derivative of E with respect to a and b to zero. Extremizing the energy E with respect to a (E_p is not a function of a), we obtain $a_0 = \alpha H b^2 / 2\sigma$. The extremum energy E_e is $E_e = -0.25\alpha^2 H^2 b^4/\sigma + E_p$. Before depinning, $E_p = 0$, the optimum b is just l, and the optimum a and $E_e = E_0$ are $a_0 = \alpha H l^2/2\sigma$ and $E_0 = -0.25\alpha^2 H^2 l^4/\sigma$, respectively. The magnetization change due to the distortion of the domain wall is proportional to $ab^2 N$ where N is the cell density. The low-field susceptibility is given by

$$\chi \propto ab^2/H \propto l^4 N/\sigma.$$

As b is increased beyond l, E_p becomes positive and E_e increases and reaches a maximum E_c which is obtained by extremizing E_e with respect to b; we get $b_c = (2V\sigma)^{0.5}/\alpha H$ and $E_c = 0.5 V b_c^2 - V l^2$. The barrier Δ for depinning is the difference $E_c - E_0$. After simplification, we obtain $\Delta = V b_c^2 (x^2 - 1)^2/2$ where $x = l/b_c$. Depinning at zero temperature occurs when $\Delta = 0$. We obtain $b_c = l$ and $H_{c0} = (2V\sigma)^{0.5}/\alpha l$. For H *close* to H_{c0}, $\Delta = l^4 \alpha^2 (H - H_c)^2/\sigma$. At finite T, depinning occurs when $\Delta/T = c$ for some constant c of the order of unity. This implies a finite-temperature switching field given by

$$H_c(T)/H_{c0} = 1 - c'(T/V)^{0.5}/l$$

at low temperatures when $H_c(T)$ is close to H_{c0}. The depinning field is replotted in this manner in figure 5. This scaling seems to be followed quite well in that results for different parameters seem to fall on the same curve. There are deviations at high temperatures, which is beyond the limit of validity of the above formula. There is also a small deviation from a complete square-root temperature dependence which may be due to additional temperature dependence of the effective coupling constants in the model.

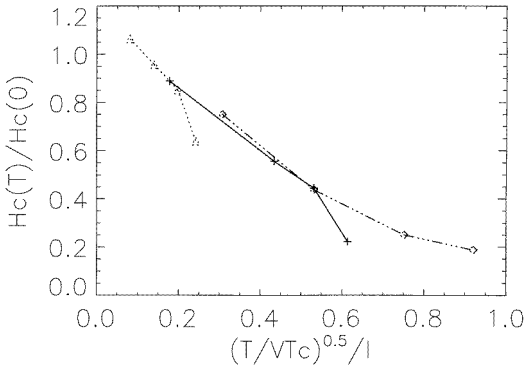

Figure 5. The data of figure 1 replotted with the temperature normalized by the boundary width l and the pinning potential V. $H_c(0)$ is the value of the switching field extrapolated to zero temperature.

Our results provide suggestions for the design of the optimum finite-temperature magnet. Larger cell boundary width l implies a slower temperature dependence but also implies a smaller zero-temperature switching field H_{c0}. Optimum operation at a specific temperature requires an optimization of the parameters V and l. From the above results, for a given pinning strength V, we obtained the optimum boundary width at the operating temperature T_{op} given by $l_0 \propto (T_{op}/V)^{0.5}$ with an optimum depinning field $H_0 \propto V\sqrt{(\sigma/T)}$.

5. Conclusions

In conclusion, we have discussed simulation and analytic results on the depinning of domain boundaries from 3D cell defects. The agreement between the analytic and the numerical results is reasonable. Our results are qualitatively different from those for pinning by 2D defects. As the cell boundary width is increased, the depinning field approaches zero in the present case, whereas for 2D defects, they saturate at a finite value. The temperature dependence of the switching field can change from fast to slow as the pinning potential is increased. This suggests that for better 2:17 magnets, one needs narrower cell boundaries and a bigger difference in anisotropies and exchanges between the boundary and the bulk. The optimum magnet at room temperature possesses an optimum l that is different from that for the optimum magnet at high temperatures.

Experimentally, the cell size can be changed. This will change the density of the nucleation centres but to the zeroth order will not change the nucleation barrier. Thus we think that the cell size is not as crucial a rate-limiting factor as the cell boundary width. Our analytic calculation can be improved to take into account the finite-temperature fluctuation of the walls in a more realistic manner. The problem here bears a resemblance to the wetting problem [3, 5]. The methods developed there may be applicable here.

Acknowledgments

The author thanks G C Hadjipanayis for helpful conversations. This work was supported in part by the AFOSR under contract F49620-96-1-0434 and by the ONR under contract N00014-97-1-0300.

References

[1] Chui S T 1995 *Phys. Rev.* B **51** 250
[2] Chui S T and Weeks J D 1980 *Phys. Rev.* B **21** 4413
Near the onset of depinning, most of the curvature of the domain wall occurs inside the cell boundaries. Hence the anisotropy inside the boundaries appears in this formula.
[3] Forgacs G, Lipowsky R and Nieuwenhuizen Th M 1990 *Phase Transitions and Critical Phenomena* ed C Domb and J Lebowitz (New York: Academic)
[4] Chaiken P and Lubensky T 1995 *Principles of Condensed Matter Physics* (Cambridge: Cambridge University Press)
[5] Chui S T and Weeks J D 1981 *Phys. Rev.* B **23** 2438
[6] Nesbitt E A, Willens R H, Sherwood R C, Buehler F and Wernick J H 1968 *Appl. Phys. Lett.* **12** 361
[7] See Strnat K J 1988 *Ferromagnetic Materials* vol 4, ed E P Wohlfarth and K H J Buschow (New York: North-Holland) p 134
[8] Kim A 1998 unpublished
[9] Liu J F, Chui S T, Dimitrov D and Hadjipanayis G C 1998 *Appl. Phys. Lett.* **73** 3007
[10] Liu J F, Zhang Y, Ding Y, Dimitrov D and Hadjipanayis G C 1998 *Proc. 15th Int. Workshop on Rare Earth Permanent Magnets (Dresden, Germany)* (Berlin: Springer)
[11] Chen X, Liu J F, Ni C, Hadjipanayis G C and Kim A 1998 *J. Appl. Phys.* **83** 7139

[12] The value used is for Heisenberg magnets with zero anisotropy. We have performed simulations with the appropriate value of the anisotropy constant and found that a more accurate $T_c = 1.7J$. We expect slight variations of the parameters from sample to sample and thus consider very accurate estimates not necessary at this stage.

[13] Livingston J D and Martin D L 1977 *J. Appl. Phys.* 1350

[14] Paul D I 1979 *J. Appl. Phys.* **50** 2128
Paul D I 1982 *J. Appl. Phys.* **53** 2362 and references therein

[15] See, for example, Chui S T 1997 *Magnetic Hysteresis in Novel Magnetic Material (NATO ASI Series E, vol 338)* ed G C Hadjipanayis (Dordrecht: Kluwer)

[16] See, for example, Schrefl T, Fischer R, Fidler J and Kronmuller H 1994 *J. Appl. Phys.* **76** 7053

[17] See, for example, Fidler J 1997 *Magnetic Hysteresis in Novel Magnetic Materials (NATO ASI Series E, vol 338)* ed G C Hadjipanayis (Dordrecht: Kluwer)

[18] Katter M 1998 *J. Appl. Phys.* **83** 6721 and references therein

[19] See, for example, Binder K and Heermann D W 1992 *Monte Carlo Simulation in Statistical Physics* (Berlin: Springer)

[20] Chui S T and Tian D C 1995 *J. Appl. Phys.* **78** 3965
Chui S T 1995 *J. Appl. Phys.* **79** 4951
Chui S T 1997 *Phys. Rev.* B **55** 3688
Chui S T 1997 *J. Magn. Magn. Mater.* **168** 9
Chui S T 1996 *Appl. Phys. Lett.* **68** 3641
Chui S T 1997 *Phys. Rev. Lett.* **78** 2224
Chui S T 1998 *J. Magn. Magn. Mater.* 177 1303
Chui S T and Ryzhov V N 1998 *J. Magn. Magn. Mater.* **182** 25